Optics Letters

High-resolution real-time 360° 3D model reconstruction of a handheld object with fringe projection profilometry

Jiaming Qian,[1,2,3] Shijie Feng,[1,2,3] Tianyang Tao,[1,2,3] Yan Hu,[1,2,3] Kai Liu,[1,2,3] Shuaijie Wu,[1,2,3] Qian Chen,[1,2,4] and Chao Zuo[1,2,3,*]

[1]School of Electronic and Optical Engineering, Nanjing University of Science and Technology, No. 200 Xiaolingwei Street, Nanjing, Jiangsu Province 210094, China
[2]Jiangsu Key Laboratory of Spectral Imaging & Intelligent Sense, Nanjing University of Science and Technology, Nanjing, Jiangsu Province 210094, China
[3]Smart Computational Imaging (SCI) Laboratory, Nanjing University of Science and Technology, Nanjing, Jiangsu Province 210094, China
[4]e-mail: chenqian@njust.edu.cn
*Corresponding author: zuochao@njust.edu.cn

Received 10 October 2019; revised 27 October 2019; accepted 28 October 2019; posted 29 October 2019 (Doc. ID 379889); published 27 November 2019

The digitization of the complete shape of real objects has essential applications in fields of intelligent manufacturing, industrial detection, and reverse modeling. In order to build the full geometric models of rigid objects, the object must be moved relative to the measurement system (or the scanner must be moved relative to the object) to obtain and integrate views of the object from all sides, which not only complicates the system configuration but makes the whole process time-consuming. In this Letter, we present a high-resolution real-time 360° three-dimensional (3D) model reconstruction method that allows one to rotate an object manually and see a continuously updated 3D model during the scanning process. A multi-view fringe projection profilometry system acquires high-precision depth information about a handheld object from different perspectives and, meanwhile, the multiple views are aligned and merged together in real time. Our system employs stereo phase unwrapping and an adaptive depth constraint that can unwrap the phase of dense fringe images robustly without increasing the number of captured patterns. We then develop an efficient coarse-to-fine registration strategy to match the 3D surface segments rapidly. Our experiments demonstrate that our method can reconstruct the high-precision complete 3D model of complex objects under arbitrary rotation without any instrument assist and expensive pre/post-processing.

https://doi.org/10.1364/OL.44.005751

Optical non-contact three-dimensional (3D) shape measurement techniques have been widely used in industrial inspection, intelligent manufacturing, reverse engineering, and many other aspects [1]. Fringe projection profilometry (FPP) [2,3] is one of the most popular 3D imaging technologies due to high measurement accuracy, simple hardware configuration, and flexibility in implementation. So far, most researches on FPP are focused on 3D measurement from a single perspective [4–6]. However, in applications such as industrial inspection and reverse modeling, it is essential to acquire all 3D models of objects. However, a conventional FPP system cannot obtain an entire 3D model of the target in single measurement due to its limited field of view, the acquisition of which requires registration of data measured from multiple views.

To obtain and align 3D shapes of the object from different views, instrument assistance is usually required to perform 3D registration [7–9]. Common auxiliary instruments include rotary stages, robotic arms, and plane mirrors. By rotary stage, multi-frame point clouds can be converted to the same coordinate system through the relationship between the rotation of the rotary stage axis and the imaging system [7]. However, the object can only be rotated around the rotary stage axis; thus, obtaining the 3D data of top and bottom is inconvenient. Robotic arms can acquire information from more perspectives by presetting a moving path [8]. However, the cost of robotic arms is high, the system assisted by which needs complex hardware connection, so implementing such systems is difficult. Measurement systems with two mirrors can reconstruct a panoramic 3D surface in one measurement, since they simultaneously capture the target from three perspectives [9]. However, such systems are still unable to acquire full-scale 3D measurements due to limited perspective information.

The aforementioned instrument-assisted registration methods are not the ideal means to obtain a 360° 3D model because of expensive hardware facilities, complicated structures, or limited perspective information. The ideal way is to rotate objects arbitrarily for 3D data of enough perspectives while sequentially performing real-time 3D registration. So far, few people have reported such methods because (1) constructing real-time, high-precision 3D measurement system based on FPP for

dynamic objects is hard due to the limitation of hardware technologies and real-time algorithms [4,10]; (2) uninterrupted real-time high-precision 3D registration without auxiliary instruments is very challenging [11]. In 2002, Rusinkiewicz *et al.* [12] proposed a real-time 3D model acquisition method based on a structured-light rangefinder and a real-time variant of the iterative closest point (ICP) algorithm. Compared with previous approaches, it permits users to rotate an object by hand and see a continuously updated model, thus providing instant feedback about the holes presence and the surface that has been covered. However, the point clouds acquired by a stripe boundary coding strategy is rather sparse, making the 3D data accumulation process less efficient. Besides, the accuracy of their registration method is low, since they skip the conventional instrument-assisted coarse registration and directly perform the variant-ICP-based fine registration without a good pose estimation. Thus, time-consuming post-processing is required for reconstructing a high-precision 3D model.

In this Letter, we realize the real-time acquisition of 360° 3D model of the object with overall accuracy up to 100 μm level without any instrument assistance for the first time, to the best of our knowledge. With our method, one can rotate the object arbitrarily by hand. As the object's 3D data from a single perspective is acquired, it can be automatically registered with that of the previous frame in real time and merged together to create a high-precision 3D model.

In order to achieve real-time 3D registration, 3D data of each perspective have to be acquired in real time. The two mainstream fringe analysis methods of FPP are Fourier-transform profilometry [13,14] with single-shot nature and phase-shifting profilometry (PSP) [15], well known for higher measurement resolution and precision. Considering the accuracy, the latter technology is chosen. Since motion will cause phase errors between frames and break the basic assumptions of PSP, PSP with as few fringe patterns as possible should be employed. Therefore, three-step phase-shifting method is used. With three-step phase-shifting patterns, the wrapped phase of the object can be easily obtained. To unwrap the phase, a conventional method is to use the temporal phase-unwrapping technologies [16]. However, a large number of auxiliary fringe patterns are required, which increases the sensitivity to motion. In this Letter, we employ the stereo phase-unwrapping (SPU) [17,18] method to eliminate phase ambiguity without using any additional auxiliary patterns.

The principle of SPU is shown in Fig. 1. For an arbitrary point o^{c_1} in Camera 1, it has N possible absolute phases, with which N 3D candidates can be reconstructed by Camera 1 and the projector. These 3D candidates can be projected onto Camera 2 to get N 2D candidates, among which there must be a correct matching point with the most similar wrapped phase to o^{c_1}. Then the phase similarity check is performed to find the matching point, and the wrapped phase of o^{c_1} can also be unwrapped. However, SPU cannot robustly remove phase ambiguity because, under the influence of noise and system error, the wrong candidate may have the phase closer to o^{c_1} than the correct point, and the higher the fringe frequency, the more likely this situation will happen. The adaptive depth constraint (ADC) [19] strategy can provide a pixel-wise depth range through the real-time measurement results, with which incorrect 3D candidates will be largely excluded. Thus, we use ADC to improve the stability of SPU.

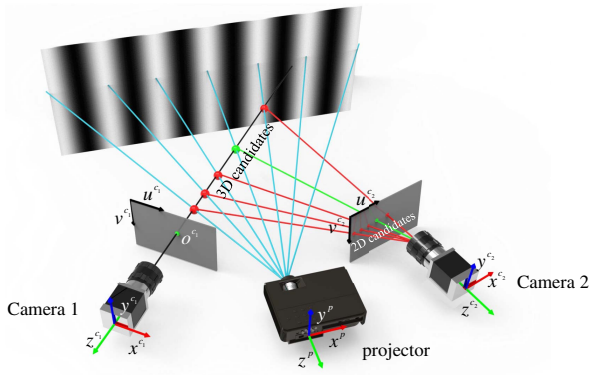

Fig. 1. Principle of SPU.

Next, we will discuss real-time high-precision 3D registration. There are two registration schemes: (1) perform fine registration directly and (2) perform fine registration after coarse registration. The first aspect focuses on the direct use of an ICP algorithm [20] and its improved variants. However, due to the lack of suitable initial pose estimation, the ICP does not work well. Besides, the ICP is usually time-consuming for higher registration accuracy and is inappropriate for real-time scenarios. The second aspect is to carry out coarse registration to estimate a good initial pose for the ICP so that the iteration can converge to the correct registration result faster with higher precision, which is a more suitable solution. However, without instrument assistance, it is not simple to perform fast coarse registration. In this Letter, we improve the simultaneous localization and mapping (SLAM) algorithm [21], which is used for localization and map construction of robots, to perform coarse registration. Define two adjacent 3D frames as Frame1 and Frame2, which have corresponding 2D texture maps I_1 and I_2, and 3D data (x_c^1, y_c^1, z_c^1) and (x_c^2, y_c^2, z_c^2) defined in a camera coordinate system. First, the key points of I_1 and I_2 are obtained and matched by scale invariant feature transformation (SIFT) [22] algorithm. The extraction of 2D features is an important step in the SLAM algorithm, making the rapid pose estimation possible since it is faster than the 3D feature extraction. Then the Euclidean distance is utilized to remove some wrong matching pairs. The matching points detected with SIFT and Euclidean distance are shown in Fig. 2(a). Among these points, there may be still some errors, as shown by those circled by red, green, and blue circles in Fig. 2(a). These wrong matching points can be eliminated by their 3D information. We record sets of 3D matching points corresponding to the found 2D ones as $P = \{P_i\}$ and $Q = \{Q_i\}$, where $i \in [1, n]$, and n is the number of matching pairs. We calculate the distance between each P_i and all elements of P. The distance set of P_i is represented as $H_i(P_i) = \{H_i(P_i, P_j)\}$, where

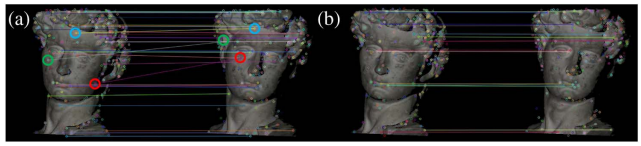

Fig. 2. Detected 2D matching points with (a) the matching points detected by the SIFT method and Euclidean distance. (b) Detected matching points optimized by our method.

$H_i(P_i, P_j)$ denotes the distance from P_i to P_j, and $j \in [1, n]$. Similarly, the distance set of Q_i is expressed as $H_i(Q_i)$. Then we obtain the difference between the corresponding elements in $H_i(P_i)$ and $H_i(Q_i)$. The difference set is represented as $D_i = \{D_{ij}\}$ and $D_{ij} = H_i(P_i, P_j) - H_i(Q_i, Q_j)$. Comparing the absolute value of each element $|D_{ij}|$ with a certain threshold value $D_{\text{thre}} = 5$ mm, if the number of elements whose absolute value is greater than D_{thre} is more than $n/2$, the point pairs P_i and Q_i are considered unreliable. With our method, the wrong matching points can be basically removed, as shown in Fig. 2(b).

After the rapid identification of 2D matching points, the transformation matrices between adjacent 3D frames can be quickly obtained with the method of solving the Perspective-n-Point (PnP) problem, which is a commonly used technology of estimating camera pose from n correspondences between 3D reference points. The conventional PnP problem in acquiring the camera pose is shown in Fig. 3(a), which is when the camera moves while the object remains stationary and the object's 3D data in the world coordinate system and its pixel coordinates when the camera moves to Position 2 are known. In this Letter, the PnP problem can be considered as how to solve the transformation matrices of moving object when the imaging system is stationary, and 3D data before the object moves and the pixel coordinates after it moves are known, as shown in Fig. 3(b). We employ the EPnP method [23], which is the non-iterative solution to a PnP problem and is widely used in visual SLAM systems due to its balance of precision and efficiency to solve the PnP problem by at least four sets of matching points.

After obtaining transformation matrixes, (x_c^1, y_c^1, z_c^1) can be registered coarsely with (x_c^2, y_c^2, z_c^2). Then we employ the ICP algorithm [20] to operate fine registration. The results after coarse and fine registrations are shown in Fig. 4. Figure 4 shows that the two point clouds represented by red and green are not registered accurately after coarse registration, while they are well aligned after fine registration. However, the ICP is unsuitable for real-time scenarios due to time-consuming iteration. To improve registration efficiency, we develop a dual-thread parallel processing mechanism, in which SLAM-based coarse registration and ICP-based fine registration can be carried out simultaneously in two separate threads. To make two registrations that should be performed serially be processed in parallel, we quantify the object motion at each coarse registration with the sum of the two norms of rotation and translation vectors obtained during coarse registration. When the motion amount is less than 30, we discard the coarse registration result and perform the next one; when it is greater than 50, considering the excessive registration error, the coarse registration will not be performed unless one rotates the object back to the position, the motion between which it and the last effective 3D frame is between 30 and 50. The ICP, which is run in a separate thread, will not be carried out until the cumulative motions $\sum m_k$ (m_k is the motion amount at the kth coarse registration) reach a certain threshold $Th_k = 200$. To improve the fine registration efficiency, 3D point clouds that have been roughly registered are first downsampled. Then the ICP algorithm is employed to the downsampled data. After deriving transformation matrices, we operate on the original dense data to finally complete fine 3D registration. The entire process of real-time 3D registration is shown in Fig. 5. Step 1: find 2D matching points with SIFT algorithm and optimize them using corresponding 3D data; Step 2: obtain the transformation matrices with the EPnP method; Step 3: register point clouds coarsely in coarse registration thread and retain the results whose motion is between 30 and 50; Step 4: if the cumulative motion reaches the threshold, execute ICP algorithm after downsampling in the fine registration thread to achieve the accurate alignment of point clouds; Step 5: return to Step 1 and repeat the above processes.

To verify the effectiveness of our algorithm, we construct a quad-camera 3D imaging system, including a LightCrafter 4500Pro (100 Hz speed), three Basler acA640-750um cameras (640 × 480 resolution) for SPU and a Basler acA640-750uc camera for colorful texture. Forty-eight-period PSP fringes are used. We use a HP Z230 computer (Intel Xeon E3-1226 v3 CPU, NVIDIA Quadro K2200 GPU) to develop our algorithm based on OpenCV and PCL. The interface of our software system is developed with Qt. The imaging speed of the system is 45 Hz, and the single scanning accuracy is 45 μm.

In the first experiment, we arbitrarily rotate the David model and realize its 360° modeling. The registration results and scenes over different time periods are shown in Fig. 6. The time for single coarse and fine registrations is 0.4 s and 2 s, respectively. The reconstruction time of the entire model

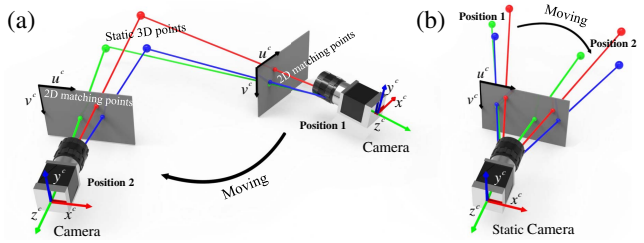

Fig. 3. Description of (a) a conventional PnP problem and (b) the problem in this Letter.

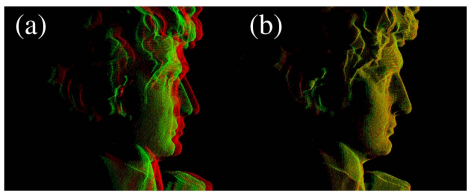

Fig. 4. Results after (a) coarse and (b) fine registrations.

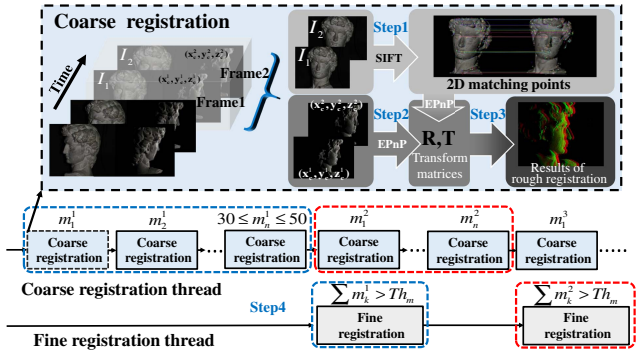

Fig. 5. Entire process of real-time 3D registration.

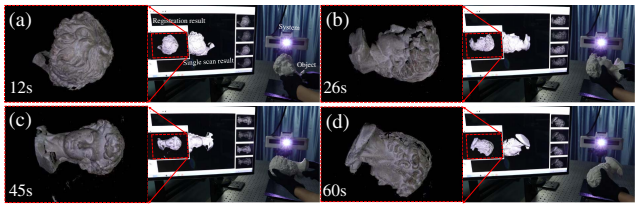

Fig. 6. Registration results and scenes of the David model over different time periods (see Visualization 1 for the whole process).

Fig. 7. Results of the David model after registration. (a) Point cloud results. (b) Triangulation results of (a).

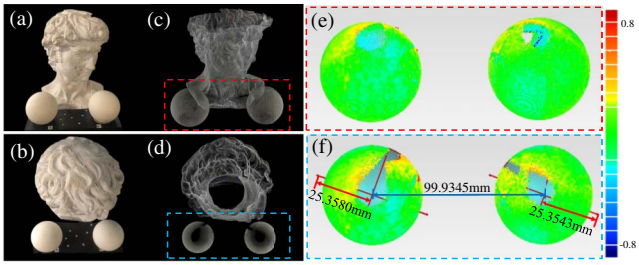

Fig. 8. Registration results of the David model and ceramic spheres. (a), (b) Measured objects from two perspectives. (c), (d) Registration results corresponding to (a), (b). (e), (f) Error distributions of the sphere registration results.

is 70 s. Figure 7 shows the results after registration, from which we can see that all 3D shapes of the David model are well aligned. This experiment demonstrates that our method can obtain a high-quality 360° 3D model of handheld objects in real time.

In the second experiment, two ceramic spheres with radii of 25.3989 and 25.4038 mm and a center-to-center distance of 100.0532 mm are measured. As spheres have no 2D features, they are registered with the aid of the David model. The measurement result is shown in Fig. 8. The sphere fitting is performed to the measured results of two spheres. Their error distributions are shown in Figs. 8(e) and 8(f). The radii of the entire reconstructed spheres are 25.3580 and 25.3543 mm, with deviations of 40.9 μm and 49.5 μm. The measured center-to-center distance is 99.9345 mm, with an error of 118.7 μm. This experiment shows that the overall accuracy of the entire 3D model reconstructed by our method can reach 100 μm level.

In summary, we have presented a high-resolution real-time 360° 3D model reconstruction technology for a handheld object with FPP for the first time, to the best of our knowledge. Compared with previous conventional complex, time-consuming 3D model acquisition systems assisted by mechanical structures, our design permits users to rotate the object by hand and see a continuously updated model as the object is scanned. Finally, a complete 3D model with accuracy up to 100 μm level can be obtained. This Letter makes low-cost, high-speed, high-precision, arbitrarily automatic 3D registration, fast-feedback and easy-to-use omni-directional 3D real-time modeling possible. We believe that this Letter will open a new door for 360° industrial inspection and rapid reverse molding and have great prospects for immensely promising applications.

Funding. National Natural Science Foundation of China (11574152, 61705105, 61722506); National Key R&D Program of China (2017YFF0106403); Outstanding Youth Foundation of Jiangsu Province of China (BK20170034); Fundamental Research Funds for the Central Universities (30917011204, 30919011222); Open Research Fund of Jiangsu Key Laboratory of Spectral Imaging Intelligent Sense (3091801410411).

Disclosures. The authors declare no conflicts of interest.

REFERENCES

1. J. Salvi, S. Fernandez, T. Pribanic, and X. Llado, Pattern Recogn. **43**, 2666 (2010).
2. J. Geng, Adv. Opt. Photon. **3**, 128 (2011).
3. S. Zhang, Opt. Lasers Eng. **106**, 119 (2018).
4. S. Zhang, Opt. Lasers Eng. **48**, 149 (2010).
5. Z. Zhang, Opt. Lasers Eng. **50**, 1097 (2012).
6. S. Feng, Q. Chen, G. Gu, T. Tao, L. Zhang, Y. Hu, W. Yin, and C. Zuo, Adv. Photonics **1**, 025001 (2019).
7. X. Liu, X. Peng, H. Chen, D. He, and B. Z. Gao, Opt. Lett. **37**, 3126 (2012).
8. M. Nießner, M. Zollhöfer, S. Izadi, and M. Stamminger, ACM Trans. Graph. **32**, 169 (2013).
9. B. Chen and B. Pan, Measurement **132**, 350 (2019).
10. J. Qian, T. Tao, S. Feng, Q. Chen, and C. Zuo, Opt. Express **27**, 2713 (2019).
11. S. Kahn, U. Bockholt, A. Kuijper, and D. W. Fellner, Comput. Ind. **64**, 1115 (2013).
12. S. Rusinkiewicz, O. Hall-Holt, and M. Levoy, ACM Trans. Graph. **21**, 438 (2002).
13. X. Su and Q. Zhang, Opt. Lasers Eng. **48**, 191 (2010).
14. L. Huang, Q. Kemao, B. Pan, and A. K. Asundi, Opt. Lasers Eng. **48**, 141 (2010).
15. C. Zuo, S. Feng, L. Huang, T. Tao, W. Yin, and Q. Chen, Opt. Lasers Eng. **109**, 23 (2018).
16. C. Zuo, L. Huang, M. Zhang, Q. Chen, and A. Asundi, Opt. Lasers Eng. **85**, 84 (2016).
17. T. Weise, B. Leibe, and L. Van Gool, in *IEEE Conference on Computer Vision and Pattern Recognition* (IEEE, 2007), pp. 1–8.
18. T. Tao, Q. Chen, J. Da, S. Feng, Y. Hu, and C. Zuo, Opt. Express **24**, 20253 (2016).
19. T. Tao, Q. Chen, S. Feng, J. Qian, Y. Hu, L. Huang, and C. Zuo, Opt. Express **26**, 22440 (2018).
20. P. J. Besl and N. D. McKay, Proc. SPIE **1611**, 586 (1992).
21. R. Mur-Artal, J. M. M. Montiel, and J. D. Tardos, IEEE Trans. Robot. **31**, 1147 (2015).
22. D. G. Lowe, Int. J. Comput. Vis. **60**, 91 (2004).
23. V. Lepetit, F. Moreno-Noguer, and P. Fua, Int. J. Comput. Vis. **81**, 155 (2009).